# LOW-FREQUENCY MODE TRANSITION IN THE FREE IN-PLANE VIBRATION OF CURVED BEAMS

T. TARNOPOLSKAYA AND F. R. DE HOOG

*CSIRO Mathematical and Information Sciences, Canberra, Australia*

AND

N. H. FLETCHER

*Research School of Physical Sciences and Engineering, Australian National University, Canberra, Australia*

The low-frequency mode transition in the free in-plane vibration of beams with varying curvature and cross-section is examined by using perturbation analysis. A simplified zeroth order equation for beam vibration in the region of the mode transition is derived. This equation shows explicitly which modes undergo a transition for a particular type of beam curvature and cross-section. Analytic approximations for frequency and mode shape are derived by the cases of beam curvature represented by symmetric and antisymmetric polynomials and their validity is illustrated by comparison with numerical solutions. Many features of mode transition phenomenon are revealed analytically, including the effect of beam curvature on mode shape during the transition stage. The similarities and distinctions between the low mode and the high mode number transitions are discussed.

© 1999 Academic Press

## 1. INTRODUCTION

Vibration of curved beams with varying cross-section has continued to attract the attention of researchers over the last two decades [1–11]. A phenomenon of transition of modes from extensional into inextensional, which occurs with increase in beam curvature, has been observed by several authors [7–9]. The possibility of the interpretation of this phenomenon in terms of two separate approximate theories (membrane and flexural vibration of a straight beam) has been suggested in reference [10], where the vibration of a particular case of an S-shaped strip of uniform cross-section has been studied. The first comprehensive study of the mode transition phenomenon in vibration of beams with arbitrarily varying curvature and cross-section is given in reference [11] on the basis of asymptotic analysis. This study revealed that for beams with hinged or clamped ends, with increasing curvature some modes undergo the transition from the flexural mode of a straight beam, through an extensional stage, into an inextensional mode, the frequency and

mode shape of which is closely approximated by those of the next higher mode of the same symmetry of a straight beam. During the stage of extensional transition, the frequency is approximated by the frequency of the associated membrane vibration problem, while the mode shape is a superposition of the mode shape of a membrane and the mode shape of flexural vibration of a straight beam. However, the asymptotic analysis presented in reference [11] is essentially limited to high mode-number vibration and therefore the results of the analysis are not applicable to the lower region of the spectrum.

In the present paper, we examine the vibrational behaviour of beams with arbitrarily varying curvature and cross-section in the lower region of the spectrum. We develop an approach which allows a simplification of the equations of free vibrations of a curved beam with varying cross-section in the low region of the spectrum and illuminates many features of the mode transition phenomenon. Thus, for example, we derive an approximate zeroth order equation of beam vibration which shows explicitly whether or not the mode transition takes place for a particular type of beam curvature and cross-section.

In the case of beams with uniform cross-section and arbitrarily varying curvature, the zeroth order equation also explicitly reveals the effect of beam curvature on mode shape during the transition stage. This equation is sufficiently simple to make an analytical solution possible for specific types of beam curvature, and we illustrate the derivation of analytic approximations for frequency and mode shape by the example of beams with curvature function represented by symmetric and antisymmetric polynomials. We then use these analytic approximations to study the vibrational behaviour in the region of mode transition and establish the similarities and distinctions between the high and the low mode-number vibrational behaviour.

For thicker beams, higher order approximations are required to describe the completion of the transition stage, and we illustrate the derivation of a first order analytic approximation by the example of a beam with constant curvature. Finally, we demonstrate the validity of the derived approximations by comparison with numerical simulations for specific types of beam curvature.

## 2. GOVERNING EQUATIONS

Consider the equations of the free in-plane vibration of a beam with arbitrarily varying curvature and cross-section [11]

$$-\bar{\varepsilon}\{-[I\bar{\kappa}^2(u'-\bar{\kappa}v)]' + \bar{\kappa}[\bar{\kappa}I(u'-\bar{\kappa}v)]'$$
$$+[\bar{\kappa}I(v'+\bar{\kappa}v)']' - \bar{\kappa}[I(v'+\bar{\kappa}u)']'\} + [\bar{A}(u'-\bar{\kappa}v)]' + \lambda\bar{A}u = 0, \tag{1}$$
$$-\bar{\varepsilon}\{-[I\bar{\kappa}^3(u'-\bar{\kappa}v) - [\bar{\kappa}I(u'-\bar{\kappa}v)]'' + \bar{\kappa}^2I(v'+\bar{\kappa}u)' + [I(v'+\bar{\kappa}u)']''\}$$
$$+\bar{A}(u'-\bar{\kappa}v)\bar{\kappa} + \lambda\bar{A}v = 0, \tag{2}$$

where $u$ and $v$ are non-dimensional longitudinal and transverse displacements, $\bar{\kappa} = \kappa l$, $\kappa$ is the curvature and $l$ is the length of the beam, $\bar{A} = A/(h_0 d_0)$, $A$ is the cross-sectional area of the beam, $h_0$ and $d_0$ are the characteristic dimensions of

the cross-section in the plane of initial curvature and in the normal plane respectively, $I = \int_{\bar{A}} \bar{z}^2 \, d\bar{A}$, $\bar{z} = z/h_0$, $z$ is the co-ordinate measured along the normal to the centreline of the beam, $\bar{\varepsilon}$ is the slenderness parameter of the beam and $\lambda$ is non-dimensional eigenvalue

$$\bar{\varepsilon} = \frac{h_0^2}{l^2}, \qquad \lambda = \frac{\rho l^2 \omega^2}{E}.$$

The primes denote differentiation with respect to the non-dimensional co-ordinate $\bar{s} = s/l$ measured along the beam centreline. If we introduce the following scaling

$$\Lambda = \frac{\lambda}{\varepsilon}; \qquad \hat{\kappa} = \frac{\bar{\kappa}}{\sqrt{\varepsilon}}; \qquad \bar{u} = \frac{u}{\sqrt{\varepsilon}}, \tag{3}$$

where $\varepsilon = \bar{\varepsilon}/12$, then equations (1) and (2) can be rewritten as

$$-\varepsilon\{-\varepsilon[I\hat{\kappa}^2(\bar{u}' - \hat{\kappa}v)]' + \varepsilon\hat{\kappa}[\hat{\kappa}I(\bar{u}' - \hat{\kappa}v)]' + [\hat{\kappa}I(v' + \varepsilon\hat{\kappa}\bar{u})']'$$

$$-\hat{\kappa}[I(v' + \varepsilon\hat{\kappa}\bar{u})']'\} + \frac{1}{12}[\bar{A}(\bar{u}' - \hat{\kappa}v)]' + \frac{\varepsilon}{12}\Lambda\bar{A}u = 0, \tag{4}$$

$$\varepsilon^2 I\hat{\kappa}^3(\bar{u}' - \hat{\kappa}v) + \varepsilon[\hat{\kappa}I(\bar{u}' - \hat{\kappa}v)]'' - \varepsilon\hat{\kappa}^2 I(v' + \varepsilon\hat{\kappa}\bar{u})'$$

$$-\{I(v' + \varepsilon\hat{\kappa}\bar{u})'\}'' + \frac{\bar{A}}{12}\hat{\kappa}(\bar{u}' - \hat{\kappa}v) + \frac{1}{12}\Lambda\bar{A}v = 0. \tag{5}$$

In the present paper, we consider the behaviour of the eigenvalues and eigenfunctions as the non-dimensional curvature $\bar{\kappa}$ of the beam gradually increases. For this purpose, it is convenient to introduce a one-parameter family of curvature functions of the form

$$\kappa = bK(\bar{s}),$$

where the parameterization is defined by $b$ and the functions $K(\bar{s})$ is fixed. Then, $\bar{\kappa} = \bar{b}K(\bar{s})$, $\hat{\kappa} = \hat{b}K(\bar{s})$, where $\bar{b} = bl$ and $\hat{b} = \bar{b}/\sqrt{\varepsilon}$. We assume that an appropriate normalization condition for eigenfunctions is chosen so that $v = O(1)$. Estimates for the order of magnitude of the terms in equations (4) and (5) can then be obtained on the basis of the results described in reference [11], namely

$$\hat{\kappa} \sim O(\varepsilon^{-1/2}), \qquad \Lambda \sim O(\hat{\kappa}^2), \qquad \bar{u} \sim O(\hat{\kappa}^{1/2}).$$

The number of oscillations in the non-dimensional amplitude of transverse and longitudinal displacements is of the order $\hat{\kappa}^{1/2}$. Taking the above into account and separating out the parts of the same order of magnitude in each term of equations (4) and (5) yield

$$\chi^2[IK^2(\bar{u}' - \hat{\kappa}v)]' - \chi^2 K[KI(\bar{u}' - \hat{\kappa}v)]' - \chi[KI(v' + \chi K\bar{u})']'$$

$$+ K\chi[I(v' + \chi K\bar{u})']' + \frac{1}{12}[\bar{A}(\bar{u}' - \hat{\kappa}v)]' + \frac{\chi}{12\hat{b}}\Lambda\bar{A}\bar{u} = 0, \tag{6}$$

$$\chi^2 I\hat{b}K^3(\bar{u}' - \hat{\kappa}v) + \chi[KI(\bar{u}' - \hat{\kappa}v)]'' - \chi\hat{b}IK^2(v' + \chi K\bar{u})'$$

$$- [I(v' + \chi K\bar{u})']''\} + \frac{\bar{A}}{12}\hat{\kappa}(\bar{u}' - \hat{\kappa}v) + \frac{1}{12}\Lambda\bar{A}v = 0, \tag{7}$$

where $\chi = \varepsilon \hat{b} = hb/\sqrt{12}$. Obviously, equations (6) and (7) contain the parameter $\chi$ which is small for relatively thin beams in the region where the mode transition takes place. In the following section, a perturbation analysis of these equations will be performed for small $\chi$.

In the present paper, we consider the boundary conditions corresponding to clamped ends, that is

$$\bar{u} = 0 \quad \text{at } \bar{s} = 0, 1, \tag{8}$$

$$v = v' = 0 \quad \text{at } \bar{s} = 0, 1. \tag{9}$$

It is straightforward, however, to modify the results for a hinged end arrangement.

## 3. PERTURBATION ANALYSIS

In the following analysis, the parameter $\chi$ is considered to be small. We use a perturbation approach to seek solution of the eigenvalue problem (6–7) of the form

$$\Lambda(\chi) = \sum_{k=0}^{\infty} \chi^k \Lambda_k, \tag{10}$$

$$\bar{u}(\bar{s}, \chi) = \sum_{k=0}^{\infty} \chi^k \bar{u}_k(\bar{s}), \tag{11}$$

$$v(\bar{s}, \chi) = \sum_{k=0}^{\infty} \chi^k v_k(\bar{s}). \tag{12}$$

Substituting these expansions into equations (6) and (7) and comparing powers of $\chi$ yields the following sequence of equations.

*zeroth order approximation*:

$$[\bar{A}(\bar{u}_0' - \hat{\kappa} v_0)]' = 0, \tag{13}$$

$$-(12 I v_0'')'' + \bar{A}\hat{\kappa}(\bar{u}_0' - \hat{\kappa} v_0) + \Lambda_0 \bar{A} v_0 = 0, \tag{14}$$

*first order approximation*:

$$-(12 I K v_0'')' + K(12 I v_0'')' + [\bar{A}(\bar{u}_1' - \hat{\kappa} v_1)]' + \frac{\bar{A}\Lambda_0 \bar{u}_0}{\hat{b}} = 0, \tag{15}$$

$$[12 I K (\bar{u}_0' - \hat{\kappa} v_0)]'' - 12 I \hat{b} K^2 v_0'' - [12 I (v_1' + K \bar{u}_0)')]''$$
$$+ \bar{A}\hat{\kappa}(\bar{u}_1' - \hat{\kappa} v_1) + \bar{A}(\Lambda_1 v_0 + \Lambda_0 v_1) = 0. \tag{16}$$

The solutions must all satisfy the boundary conditions

$$\bar{u}_k(0) = \bar{u}_k(1) = 0, \tag{17}$$

$$v_k(0) = v_k(1) = 0, \tag{18}$$

$$v_k'(0) = v_k'(1) = 0, \tag{19}$$

where $k$ is the order of the approximation.

## 3.1. ZEROTH ORDER APPROXIMATION AND PROPERTIES OF MODE TRANSITION

Consider the zeroth order equations (13) and (14) with boundary conditions (17)–(19). It is convenient to rewrite equations (13) and (14) as a single equation. On integrating (13) and using the boundary condition (17) we obtain

$$\bar{A}(\bar{u}_0' - \hat{\kappa} v_0) = - \int_0^1 (\bar{A} \hat{\kappa} v_0 + \bar{A}' u_0) \, \mathrm{d}\bar{s}, \tag{20}$$

and substituting this expression into equation (14) yields

$$- (12 I v_0'')'' + \Lambda_0 \bar{A} v_0 = \hat{\kappa} \int_0^1 (\bar{A} \hat{\kappa} v_0 + \bar{A}' u_0) \, \mathrm{d}\bar{s}. \tag{21}$$

Note that equation (21) differs from the equation of vibration of a straight beam with varying cross-section by the term on the right-hand side and therefore the vibrational modes of a curved beam generally differ from those of a straight beam. The exception is the situation when

$$\int_0^1 (\bar{A} \hat{\kappa} v_0 + \bar{A}' u_0) \, \mathrm{d}\bar{s} = 0, \tag{22}$$

and in this case the frequency and mode shape of the curved beam are given, up to the zeroth order, by the corresponding functions for a straight beam. Obviously, no mode transition occurs in this case. This is the case, for example, for some modes of beams whose curvature and cross-section are symmetric or antisymmetric. Hence, condition (22) shows that in the case when both the curvature and cross-section of the beam are functions with even symmetry, the modes antisymmetric in $v$ are unaffected by curvature increase, while the modes symmetric in $v$ undergo a mode transformation. In the case when the curvature is an antisymmetric function and the cross-section is a symmetric function, the modes symmetric in $v$ remain unchanged, while the modes antisymmetric in $v$ are subject to mode transition.

In the case of a beam with varying curvature and uniform cross-section, equation (21) reduces to the scalar equation

$$- v_0'''' + \Lambda_0 v_0 = \hat{\kappa} \int_0^1 \hat{\kappa} v_0 \, \mathrm{d}\bar{s}. \tag{23}$$

The solution of equation (23) takes a form

$$v_0 = v_{0h} + v_{0p}, \tag{24}$$

where $v_{0h}$ is the solution of the homogeneous equation

$$- v_0'''' + \Lambda_0 v_0 = 0 \tag{25}$$

which represents the vibration of a straight beam, while $v_{0p}$ is a particular solution of equation (23). We can see that the transverse displacements of a curved beam during the transition stage are a superposition of a transverse displacement of a straight beam and a function depending on beam curvature. The exceptions are

the modes for which

$$\int_0^1 \hat{\kappa} v_0 \, d\bar{s} = 0, \tag{26}$$

and in this case no mode transition occurs. Obviously, for a beam whose curvature is a symmetric or antisymmetric function, only those modes possessing the same type of symmetry in the transverse component of displacement as the beam curvature function undergo a mode transition.

A particular solution of equation (23) can be obtained for specific types of beam curvature. In this paper, we consider the beam curvature represented by polynomials of degree up to 3, in which case the solution of equation (23) is particularly simple. However, it is straightforward to extend the analysis to other types of beam curvature, using the approach described below. For a beam curvature represented by a polynomial of degree up to 3, a particular solution of equation (23) is given by

$$v_{0p} = \frac{\hat{\kappa}}{\Lambda_0} \int_0^1 \hat{\kappa} v_0 \, d\bar{s} \tag{27}$$

and we can see that in this case the additional component in the transverse displacements that appears during the transition stage is proportional to the beam curvature function.

The eigenvalue problem (23) can be solved analytically for symmetric and antisymmetric curvature functions, as we illustrate below.

### 3.1.1. *Symmetric polynomial curvature function*

For clarity, we consider a beam curvature function in the form of a symmetric polynomial of up to second degree. It is straightforward, however, to extend the results of the present section to symmetric polynomials of higher degree.

In the case of a symmetric curvature function, the zeroth order approximation for the modes antisymmetric in $v$ can be obtained from the equation of vibration of a straight beam. Of interest are the modes symmetric in $v$, as such modes undergo a mode transition, and in this case the solution $v_{0h}$ of the homogeneous equation is given by

$$v_{0h} = C\{\cosh[\Lambda_0^{1/4}(\bar{s} - \tfrac{1}{2})] + C_1 \cos[\Lambda_0^{1/4}(\bar{s} - \tfrac{1}{2})]\}, \tag{28}$$

where $C$ and $C_1$ are arbitrary constants. The expression for $\int_0^1 \hat{\kappa} v_0 \, d\bar{s}$ can be found by multiplying equation (27) by $\hat{\kappa}$ and integrating it, so that

$$\int_0^1 \hat{\kappa} v_0 \, d\bar{s} = \frac{\Lambda_0 \hat{b} \int_0^1 K v_{0h} \, d\bar{s}}{\Lambda_0 - \hat{b}^2 \int_0^1 K^2 \, d\bar{s}}, \tag{29}$$

and therefore

$$v_0 = v_{0h} + \hat{b}^2 \frac{K \int_0^1 K v_{0h} \, d\bar{s}}{\Lambda_0 - \hat{b}^2 \int_0^1 K^2 \, d\bar{s}}. \tag{30}$$

The equation for the non-dimensional eigenvalue $\Lambda_0$ can be obtained by substituting the boundary conditions (18) and (19) into the last equation, which gives

$$\frac{\hat{b}^2 K(1) \int_0^1 K(\bar{s}) \left\{ \cosh \left[ \Lambda_0^{1/4} (\bar{s} - \tfrac{1}{2}) \right] + C_1 \cos \left[ \Lambda_0^{1/4} (\bar{s} - \tfrac{1}{2}) \right] \right\} d\bar{s}}{\Lambda_0 - \hat{b}^2 \int_0^1 K^2(\bar{s}) d\bar{s}}$$

$$+ \cosh \frac{\Lambda_0^{1/4}}{2} + C_1 \cos \frac{\Lambda_0^{1/4}}{2} = 0, \tag{31}$$

where

$$C_1 = \frac{K(1) \Lambda_0^{1/4} \sinh \dfrac{\Lambda_0^{1/4}}{2} - K'(1) \cosh \dfrac{\Lambda_0^{1/4}}{2}}{K(1) \Lambda_0^{1/4} \sin \dfrac{\Lambda_0^{1/4}}{2} + K'(1) \cos \dfrac{\Lambda_0^{1/4}}{2}}. \tag{32}$$

Although equation (31) cannot be solved for the non-dimensional eigenvalue $\Lambda_0$ as a function of non-dimensional curvature $\hat{b}$, it can be solved explicitly for the inverse function $\hat{b}(\Lambda_0)$

$$\hat{b}^2 = \Lambda_0 \left( \cosh \frac{\Lambda_0^{1/4}}{2} + C_1 \cos \frac{\Lambda_0^{1/4}}{2} \right) \left\{ \left( \cosh \frac{\Lambda_0^{1/4}}{2} + C_1 \cos \frac{\Lambda_0^{1/4}}{2} \right) \int_0^1 K^2(\bar{s}) d\bar{s} \right.$$

$$\left. - K(1) \int_0^1 K^2(\bar{s}) \left\{ \cosh \left[ \Lambda_0^{1/4} \left( \bar{s} - \frac{1}{2} \right) \right] + C_1 \cos \left[ \Lambda_0^{1/4} \left( \bar{s} - \frac{1}{2} \right) \right] \right\} d\bar{s} \right\}^{-1}. \tag{33}$$

Equation (33) can be further simplified by substituting a particular form of beam curvature function $K(\bar{s})$. As an example of a curvature function with even symmetry, we consider a constant curvature $K(\bar{s}) = 1$. In this case, equation (33) reduces to

$$\hat{b}^2 = \Lambda_0 \frac{\sin \dfrac{\Lambda_0^{1/4}}{2} \cosh \dfrac{\Lambda_0^{1/4}}{2} + \sinh \dfrac{\Lambda_0^{1/4}}{2} \cos \dfrac{\Lambda_0^{1/4}}{2}}{\sin \dfrac{\Lambda_0^{1/4}}{2} \cosh \dfrac{\Lambda_0^{1/4}}{2} + \sinh \dfrac{\Lambda_0^{1/4}}{2} \cos \dfrac{\Lambda_0^{1/4}}{2} - \dfrac{4}{\Lambda_0^{1/4}} \sin \dfrac{\Lambda_0^{1/4}}{2} \sinh \dfrac{\Lambda_0^{1/4}}{2}}. \tag{34}$$

This equation illustrates how the eigenvalues change with increasing non-dimensional curvature. The eigenvalues of a curved beam take on values lying between the root of the equation

$$\sin \frac{\Lambda_0^{1/4}}{2} \cosh \frac{\Lambda_0^{1/4}}{2} + \sinh \frac{\Lambda_0^{1/4}}{2} \cos \frac{\Lambda_0^{1/4}}{2} = 0, \tag{35}$$

and the horizontal asymptote defined by the nearest larger root of the equation

$$\sin \frac{\Lambda_0^{1/4}}{2} \cosh \frac{\Lambda_0^{1/4}}{2} + \sinh \frac{\Lambda_0^{1/4}}{2} \cos \frac{\Lambda_0^{1/4}}{2} - \frac{4}{\Lambda_0^{1/4}} \sin \frac{\Lambda_0^{1/4}}{2} \sinh \frac{\Lambda_0^{1/4}}{2} = 0. \tag{36}$$

The approximate value of the non-dimensional eigenvalue $\Lambda^*$ which defines a horizontal asymptote $\Lambda = \Lambda^*$ can be found by solving equation (36) under the assumption that $\Lambda_0^{-1/4}$ is small. With accuracy up to $o(\Lambda^{-1/4})$ this yields

$$\Lambda^* = \left( -\frac{\pi}{4} + \pi k + 1 \right)^4 \left[ 1 + \sqrt{1 - \frac{4}{-\pi/4 + \pi k + 1}} \right], \tag{37}$$

where $k = 2$ corresponds to the asymptote which is approached during the transition of the lowest symmetric mode. Note that the root of equation (35) represents the eigenvalue of a straight beam, while the value given by equation (37) is smaller than the next successive root of equation (35). This means that during the transition stage the eigenvalue of the curved beam increases towards, but does not reach, the eigenvalue of the next higher mode of a straight beam with the same symmetry.

We now examine how the mode shape changes during the mode transition stage. The zeroth order approximation for the transverse components of the eigenfunction $v_0$ is given by

$$v_0 = C \left\{ \sin \frac{\Lambda_0^{1/4}}{2} \cosh \left[ \Lambda_0^{1/4} \left( \bar{s} - \frac{1}{2} \right) \right] + \sinh \frac{\Lambda_0^{1/4}}{2} \cos \left[ \Lambda_0^{1/4} \left( \bar{s} - \frac{1}{2} \right) \right] \right.$$
$$\left. - \sin \frac{\Lambda_0^{1/4}}{2} \cosh \frac{\Lambda_0^{1/4}}{2} - \sinh \frac{\Lambda_0^{1/4}}{2} \cos \frac{\Lambda_0^{1/4}}{2} \right\} \tag{38}$$

and it can be seen that it differs from the normal component of the eigenfunction of a straight beam by an additive constant (last two terms in curly brackets). The value of this constant is zero at zero curvature and gradually increases with increase in non-dimensional curvature. However, when the eigenvalue approaches the asymptotes given by equation (36), the value of the constant decreases and approaches the limit $(4/\Lambda_0^{1/4}) \sin(\Lambda_0^{1/4}/2) \sinh(\Lambda_0^{1/4}/2)$. Thus, an additional component remains in the transverse displacements even on completion of the transition stage.

It is interesting to see how the magnitude of the extension varies during the transition stage. A zeroth order approximation for the tangential component of the eigenfunction can be obtained as

$$u_0 = \hat{b} \left( \int_0^{\bar{s}} v_0 \, d\bar{s} - \bar{s} \int_0^1 v_0 \, d\bar{s} \right) = \frac{\hat{b} C}{\Lambda_0^{1/4}} \left\{ \sin \frac{\Lambda_0^{1/4}}{2} \sinh \left[ \Lambda_0^{1/4} \left( \bar{s} - \frac{1}{2} \right) \right] \right.$$
$$\left. + \sinh \frac{\Lambda_0^{1/4}}{2} \sin \left[ \Lambda_0^{1/4} \left( \bar{s} - \frac{1}{2} \right) \right] + 4 \left( \frac{1}{2} - \bar{s} \right) \sin \frac{\Lambda_0^{1/4}}{2} \sinh \frac{\Lambda_0^{1/4}}{2} \right\} \tag{39}$$

and the extension can be calculated as

$$e = \sqrt{\varepsilon} (\bar{u}_0' - \hat{b} v_0) = C \hat{b} \left[ \sin \frac{\Lambda_0^{1/4}}{2} \cosh \frac{\Lambda_0^{1/4}}{2} \right.$$
$$\left. + \sinh \frac{\Lambda_0^{1/4}}{2} \cos \frac{\Lambda_0^{1/4}}{2} - \frac{4}{\Lambda_0^{1/4}} \sin \frac{\Lambda_0^{1/4}}{2} \sinh \frac{\Lambda_0^{1/4}}{2} \right]. \tag{40}$$

It can be seen that the extension tends to zero at the end of the transition stage, as the eigenvalue approaches the asymptotes given by equation (36), and is at its maximum when the eigenvalues take intermediate values between these asymptotes.

### 3.1.2. *Antisymmetric polynomial curvature function*

In a similar manner, zeroth order approximations for the eigenvalues and eigenfunctions can be obtained for the case of beam curvature represented by an antisymmetric polynomial. As before, we consider a polynomial up to third degree for simplicity. In the case of antisymmetric curvature, the modes symmetric in $v$ remain unchanged, while the modes antisymmetric in $v$ undergo the mode transition. The transverse displacements for the modes antisymmetric in $v$ are given by the expression (27) where

$$v_{0h} = C\left\{\sinh\left[\Lambda_0^{1/4}\left(\bar{s} - \tfrac{1}{2}\right)\right] - C_1 \sin\left[\Lambda_0^{1/4}\left(\bar{s} - \tfrac{1}{2}\right)\right]\right\} \tag{41}$$

and $C_1$ is given by

$$C_1 = \frac{K(1)\,\Lambda_0^{1/4}\cosh\dfrac{\Lambda_0^{1/4}}{2} - K'(1)\sinh\dfrac{\Lambda_0^{1/4}}{2}}{K(1)\,\Lambda_0^{1/4}\cos\dfrac{\Lambda_0^{1/4}}{2} - K'(1)\sin\dfrac{\Lambda_0^{1/4}}{2}}. \tag{42}$$

The equation for the non-dimensional eigenvalue has the form

$$\hat{b}^2 = \Lambda_0\left(\sinh\frac{\Lambda_0^{1/4}}{2} - C_1\sin\frac{\Lambda_0^{1/4}}{2}\right)\left\{\left(\sinh\frac{\Lambda_0^{1/4}}{2} - C_1\sin\frac{\Lambda_0^{1/4}}{2}\right)\int_0^1 K^2(\bar{s})\,d\bar{s}\right.$$

$$\left. - K(1)\int_0^1 K(\bar{s})\left\{\sinh\left[\Lambda_0^{1/4}\left(\bar{s} - \frac{1}{2}\right)\right] - C_1\sin\left[\Lambda_0^{1/4}\left(\bar{s} - \frac{1}{2}\right)\right]\right\}d\bar{s}\right\}^{-1}$$

$$\tag{43}$$

Equation (43) can be further simplified by considering a particular form of curvature function, and as an example of an antisymmetric polynomial curvature function we consider a linear antisymmetric curvature given by

$$\hat{\kappa} = \hat{b}(2\bar{s} - 1).$$

The equation for the eigenvalues (43) then takes the form

$$\hat{b}^2 = \Lambda_0\left(\sinh\frac{\Lambda_0^{1/4}}{2}\cos\frac{\Lambda_0^{1/4}}{2} - \sin\frac{\Lambda_0^{1/4}}{2}\cosh\frac{\Lambda_0^{1/4}}{2}\right)\left[\frac{1}{3}\left(\cos\frac{\Lambda_0^{1/4}}{2}\sinh\frac{\Lambda_0^{1/4}}{2}\right.\right.$$

$$\left. - \cosh\frac{\Lambda_0^{1/4}}{2}\sin\frac{\Lambda_0^{1/4}}{2}\right) - \frac{16}{\Lambda_0^{3/4}}\left(\frac{\Lambda_0^{1/4}}{2}\cosh\frac{\Lambda_0^{1/4}}{2} - \sinh\frac{\Lambda_0^{1/4}}{2}\right)$$

$$\left. \times\left(\frac{\Lambda_0^{1/4}}{2}\cos\frac{\Lambda_0^{1/4}}{2} - \sin\frac{\Lambda_0^{1/4}}{2}\right)\right]^{-1}. \tag{44}$$

A zeroth order approximation for the transverse component of the eigenfunction $v_0$ is given, up to multiplicative constant, by

$$v_0 = \left(\frac{\Lambda_0^{1/4}}{2}\cos\frac{\Lambda_0^{1/4}}{2} - \sin\frac{\Lambda_0^{1/4}}{2}\right)\sinh\left[\Lambda_0^{1/4}\left(\bar{s} - \frac{1}{2}\right)\right] - \left(\frac{\Lambda_0^{1/4}}{2}\cosh\frac{\Lambda_0^{1/4}}{2}\right.$$

$$\left. - \sinh\frac{\Lambda_0^{1/4}}{2}\right)\sinh\left[\Lambda_0^{1/4}\left(\bar{s} - \frac{1}{2}\right)\right] - (2\bar{s} - 1)\frac{\Lambda_0^{1/4}}{2}\left(\sinh\frac{\Lambda_0^{1/4}}{2}\cos\frac{\Lambda_0^{1/4}}{2}\right.$$

$$\left. - \sin\frac{\Lambda_0^{1/4}}{2}\cosh\frac{\Lambda_0^{1/4}}{2}\right), \tag{45}$$

while a zeroth order approximation for the extension is given, up to multiplicative constant, by

$$e = \hat{b}\left[-\frac{16}{\Lambda_0^{3/4}}\left(\frac{\Lambda_0^{1/4}}{2}\cos\frac{\Lambda_0^{1/4}}{2} - \sin\frac{\Lambda_0^{1/4}}{2}\right)\left(\frac{\Lambda_0^{1/4}}{2}\cosh\frac{\Lambda_0^{1/4}}{2} - \sinh\frac{\Lambda_0^{1/4}}{2}\right)\right.$$

$$\left. + \frac{1}{3}\left(\sinh\frac{\Lambda_0^{1/4}}{2}\cos\frac{\Lambda_0^{1/4}}{2} - \sin\frac{\Lambda_0^{1/4}}{2}\cosh\frac{\Lambda_0^{1/4}}{2}\right)\right]. \tag{46}$$

One can see that the features of the mode transition in the case of antisymmetric beam curvature are similar to those for symmetric curvature. With an increase in the non-dimensional curvature, the eigenvalue increases from the eigenvalue of a straight beam towards an asymptotic limit that is lower than the eigenvalue of the next mode of the straight beam with the same symmetry. The mode shape gradually transforms, with increase in non-dimensional curvature, from the mode shape for a straight beam into the mode shape that resemble that of the next higher mode of a straight beam. There is however an additional component in the transverse displacements (last term on the right-hand side of equation (45)) that is proportional to the beam curvature function and attains its maximum during the transition stage. This component then decreases as the eigenvalue approaches the asymptote and the vibration transforms into one that is nearly inextensional, but it does not disappear completely even on completion of the transition stage.

### 3.2. FIRST ORDER APPROXIMATION FOR EIGENVALUES OF BEAMS WITH UNIFORM CURVATURE

While a zeroth order approximation is sufficiently accurate throughout the transition region for thin beams ($\varepsilon \sim 10^{-6}$ and smaller), a higher order approximation is required to describe the frequency of thicker beams. In this section, we derive a first order approximation for the eigenvalues of a beam with constant curvature. In a similar manner, a first order approximation can be obtained for other types of curvature functions.

In the case of a beam with constant curvature, equations (15) and (16) take the form

$$\hat{b}(\bar{u}_1' - \hat{b}v_1)' + \Lambda_0\bar{u}_0 = 0, \tag{47}$$

$$-v_1''' - 2\hat{b}v_0'' + \hat{b}(\bar{u}_1' - \hat{b}v_1) + \Lambda_0 v_1 + \Lambda_1 v_0 = 0. \tag{48}$$

We now examine equations (47) and (48) with boundary conditions (17)–(19). Consider the eigenmodes with even symmetry in $v$, that is $\int_0^1 v \, d\bar{s} \neq 0$. On integrating equation (47) and using boundary condition (17) we obtain

$$
\bar{u}_1' - \hat{b} v_1 = -\hat{b} \int_0^1 v_1 \, d\bar{s} - C \Lambda_0^{1/2} \left\{ \frac{1}{3} \frac{\Lambda_0^{1/4}}{2} \sin \frac{\Lambda_0^{1/4}}{2} \sinh \frac{\Lambda_0^{1/4}}{2} \right.
$$
$$
+ \sin \frac{\Lambda_0^{1/4}}{2} \cosh \left[ \Lambda_0^{1/4} \left( \bar{s} - \frac{1}{2} \right) \right] - \sinh \frac{\Lambda_0^{1/4}}{2} \cos \left[ \Lambda_0^{1/4} \left( \bar{s} - \frac{1}{2} \right) \right]
$$
$$
\left. - 2 \Lambda_0^{1/4} \left( \frac{1}{2} - \bar{s} \right)^2 \sin \frac{\Lambda_0^{1/4}}{2} \sinh \frac{\Lambda_0^{1/4}}{2} \right\}. \tag{49}
$$

Substituting this last expression and the expression for $v_0$ and $v_0''$ into equation (48) gives, for $v_1$,

$$
- v_1''' + \Lambda_0 v_1 = C(3\hat{b}\sqrt{\Lambda_0} - \Lambda_1) \sin \frac{\bar{\lambda}_0^{1/4}}{2} \cosh \left[ \Lambda_0^{1/4} \left( \bar{s} - \frac{1}{2} \right) \right]
$$
$$
- C(3\hat{b}\sqrt{\Lambda_0} + \Lambda_1) \sinh \frac{\Lambda_0^{1/4}}{2} \cosh \left[ \Lambda_0^{1/4} \left( \bar{s} - \frac{1}{2} \right) \right] + \hat{b}^2 \int_0^1 v_1 \, d\bar{s}
$$
$$
+ C \frac{\Lambda_0^{3/4} \hat{b}}{6} \sin \frac{\Lambda_0^{1/4}}{2} \sinh \frac{\Lambda_0^{1/4}}{2} - 2C\Lambda_0^{3/4}\hat{b} \left( \frac{1}{2} - \bar{s} \right)^2 \sin \frac{\Lambda_0^{1/4}}{2} \sinh \frac{\Lambda_0^{1/4}}{2}
$$
$$
+ C\Lambda_1 \left( \sin \frac{\Lambda_0^{1/4}}{2} \cosh \frac{\Lambda_0^{1/4}}{2} + \sinh \frac{\Lambda_0^{1/4}}{2} \cos \frac{\Lambda_0^{1/4}}{2} \right). \tag{50}
$$

The solution can be sought as a sum of solution of the homogeneous equation $v_{h1}$ and a particular solution of equation (50) $v_{p1}$

$$
v_1 = v_{h1} + v_{p1}, \tag{51}
$$

where the solution of the homogeneous equation is given by

$$
v_{h1} = C_1 \cosh \left[ \Lambda_0^{1/4} (\bar{s} - \tfrac{1}{2}) \right] + C_2 \cos \left[ \Lambda_0^{1/4} (\bar{s} - \tfrac{1}{2}) \right] \tag{52}
$$

and $C_1$ and $C_2$ are arbitrary constants. Since equation (50) is linear, the superposition principle applies and the particular solution can be formed as a sum of particular solutions. It is easy to verify that

$$
v_{p1} = \frac{C\Lambda_1}{\Lambda_0} \left( \sin \frac{\Lambda_0^{1/4}}{2} \cosh \frac{\Lambda_0^{1/4}}{2} + \sinh \frac{\Lambda_0^{1/4}}{2} \cos \frac{\Lambda_0^{1/4}}{2} \right) + \frac{\hat{b}^2}{\Lambda_0} \int_0^1 v_1 \, d\bar{s}
$$
$$
- \frac{2C\hat{b}}{\Lambda_0^{1/4}} \left( \frac{1}{2} - \bar{s} \right)^2 \sin \frac{\Lambda_0^{1/4}}{2} \sinh \frac{\Lambda_0^{1/4}}{2} + \frac{C\hat{b}}{6\Lambda_0^{1/4}} \sin \frac{\Lambda_0^{1/4}}{2} \sinh \frac{\Lambda_0^{1/4}}{2}
$$
$$
+ \frac{C(3\hat{b}\sqrt{\Lambda_0} + \Lambda_1)}{4\Lambda_0^{3/4}} \left( \frac{1}{2} - \bar{s} \right) \sinh \frac{\Lambda_0^{1/4}}{2} \sin \left[ \Lambda_0^{1/4} \left( \bar{s} - \frac{1}{2} \right) \right]
$$
$$
+ \frac{C(3\hat{b}\sqrt{\Lambda_0} - \Lambda_1)}{4\Lambda_0^{3/4}} \left( \frac{1}{2} - \bar{s} \right) \sin \frac{\Lambda_0^{1/4}}{2} \sinh \left[ \Lambda_0^{1/4} \left( \bar{s} - \frac{1}{2} \right) \right]. \tag{53}
$$

One of the constants (for example, $C_2$) can be found from the boundary condition (19)

$$
C_2 = C_1 \frac{\sinh \frac{\Lambda_0^{1/4}}{2}}{\sin \frac{\Lambda_0^{1/4}}{2}} + \frac{C\Lambda_1 \left( \sin \frac{\Lambda_0^{1/4}}{2} \cosh \frac{\Lambda_0^{1/4}}{2} - \sinh \frac{\Lambda_0^{1/4}}{2} \cos \frac{\Lambda_0^{1/4}}{2} \right)}{8\Lambda_0^{3/4} \sin \frac{\Lambda_0^{1/4}}{2}}
$$

$$
- \frac{7C\hat{b} \sinh \frac{\Lambda_0^{1/4}}{2}}{2\sqrt{\Lambda_0}} - \frac{3C\hat{b} \left( \sin \frac{\Lambda_0^{1/4}}{2} \cosh \frac{\Lambda_0^{1/4}}{2} + \sinh \frac{\Lambda_0^{1/4}}{2} \cos \frac{\Lambda_0^{1/4}}{2} \right)}{8\Lambda_0^{1/4} \sin \frac{\Lambda_0^{1/4}}{2}} \tag{54}
$$

and $\int_0^1 v_1 \, d\bar{s}$ can be obtained by integrating equation (51)

$$
\int_0^1 v_1 \, d\bar{s} = \frac{\Lambda_0}{\Lambda_0 - \hat{b}^2} \left\{ \frac{2C_1}{\Lambda_0^{1/4}} \sinh \frac{\Lambda_0^{1/4}}{2} + \frac{5C\Lambda_1}{4\Lambda_0} \left[ \left( \sin \frac{\Lambda_0^{1/4}}{2} \cosh \frac{\Lambda_0^{1/4}}{2} \right. \right. \right.
$$

$$
\left. + \sinh \frac{\Lambda_0^{1/4}}{2} \cos \frac{\Lambda_0^{1/4}}{2} \right) - \frac{4}{5\Lambda_0^{1/4}} \sin \frac{\Lambda_0^{1/4}}{2} \sinh \frac{\Lambda_0^{1/4}}{2} \Bigg] + \frac{2C_2}{\Lambda_0^{1/4}} \sin \frac{\Lambda_0^{1/4}}{2}
$$

$$
\left. + \frac{3C\hat{b}}{4\sqrt{\Lambda_0}} \left( \sinh \frac{\Lambda_0^{1/4}}{2} \cos \frac{\Lambda_0^{1/4}}{2} - \sin \frac{\Lambda_0^{1/4}}{2} \cosh \frac{\Lambda_0^{1/4}}{2} \right) \right\}. \tag{55}
$$

We can now find the first order approximation to the eigenvalues $\Lambda_1$ by using the boundary conditions (18). This takes the form

$$
C_1 \cosh \frac{\Lambda_0^{1/4}}{2} + C_2 \cos \frac{\Lambda_0^{1/4}}{2} + \frac{\hat{b}^2}{\Lambda_0} \int_0^1 v_1 \, d\bar{s} - \frac{13C\hat{b}}{12\Lambda_0^{1/4}} \sin \frac{\Lambda_0^{1/4}}{2} \sinh \frac{\Lambda_0^{1/4}}{2}
$$

$$
+ \frac{\Lambda_1}{\Lambda_0} C \left( \sin \frac{\Lambda_0^{1/4}}{2} \cosh \frac{\Lambda_0^{1/4}}{2} + \sinh \frac{\Lambda_0^{1/4}}{2} \cos \frac{\Lambda_0^{1/4}}{2} \right) = 0. \tag{56}
$$

Substituting the expressions for $C_2$ and $\int_0^1 v_1 \, d\bar{s}$ into equation (56) and utilising equation (34) yields

$$
\Lambda_1 = \hat{b}\sqrt{\Lambda_0} \left[ 3(13\hat{b}^2 - 7\Lambda_0) \left( \sin \frac{\Lambda_0^{1/4}}{2} \cosh \frac{\Lambda_0^{1/4}}{2} - \cos \frac{\Lambda_0^{1/4}}{2} \sinh \frac{\Lambda_0^{1/4}}{2} \right) \right.
$$

$$
\left. + 13\Lambda_0^{1/4}(\Lambda_0 - \hat{b}^2) \sin \frac{\Lambda_0^{1/4}}{2} \sinh \frac{\Lambda_0^{1/4}}{2} \right] \left\{ 3 \left[ \Lambda_0^{1/4}(\Lambda_0 - \hat{b}^2) \cos \frac{\Lambda_0^{1/4}}{2} \cosh \frac{\Lambda_0^{1/4}}{2} \right. \right.
$$

$$
\left. \left. + (5\Lambda_0 + \hat{b}^2) \left( \sin \frac{\Lambda_0^{1/4}}{2} \cosh \frac{\Lambda_0^{1/4}}{2} + \sinh \frac{\Lambda_0^{1/4}}{2} \cos \frac{\Lambda_0^{1/4}}{2} \right) \right] \right\}^{-1}. \tag{57}
$$

The solution can be continued to a higher order in a similar fashion.

## 4. NUMERICAL EXAMPLES AND DISCUSSION

In this section, several numerical examples are calculated using a complete model of beam vibration (1), (2) in order to compare them with analytic solutions derived in Section 3 and validate the predictions of the theory regarding the mode transition phenomenon. The numerical results are obtained using a collocation software for boundary-value ODEs "Colnew" [14].

In Figure 1, the numerical solution for non-dimensional eigenvalues versus non-dimensional curvatures for the lowest two symmetrical modes of a beam with constant curvature is shown with solid lines. The asymptote given by equation (37) and the non-dimensional eigenvalues of the lowest two symmetric modes of a straight beam are shown by dotted lines. One can see that, as shown analytically in Section 3, with increase in non-dimensional curvature the eigenvalue increases and approaches the asymptote, which is lower than the eigenvalue of the next higher straight-beam mode with the same symmetry.
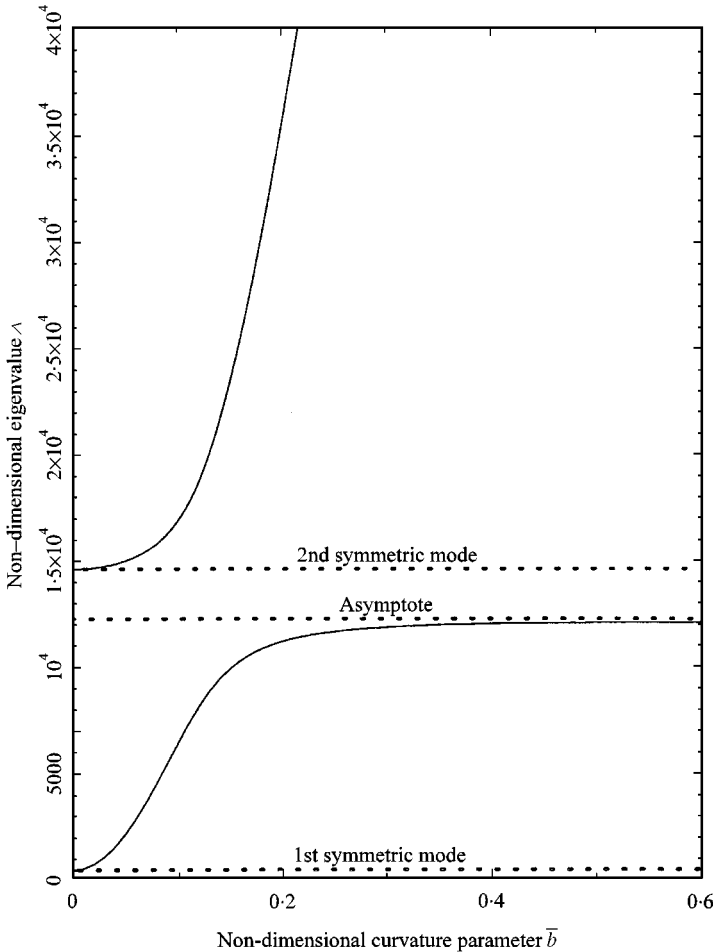


Figure 1. Non-dimensional eigenvalue $\Lambda$ of two lowest symmetric modes (———) as a function of non-dimensional curvature for a beam with constant curvature, $\varepsilon = 10^{-6}$; asymptote defined by equations (37) and eigenvalues of a straight beam are shown with dotted lines.

Figures 2 and 3 show the numerical solution (solid lines) and zeroth order approximations (dashed lines) for the eigenvalues of the lowest two modes of the beams with constant and anti-symmetric linear curvature respectively (symmetric modes are shown in the case of a beam with constant curvature and anti-symmetric modes in the other case). One can see that the zeroth order approximation gives an accurate description of the eigenvalue for the entire transition stage for beams with a thickness to length ratio of $5 \times 10^{-3}$ and smaller. Transformations of the mode shape are also shown in these figures. We can see that, as predicted, the mode gradually transforms from the flexural mode of a straight beam into the one that resembles the next higher flexural mode (with the same symmetry) of a straight
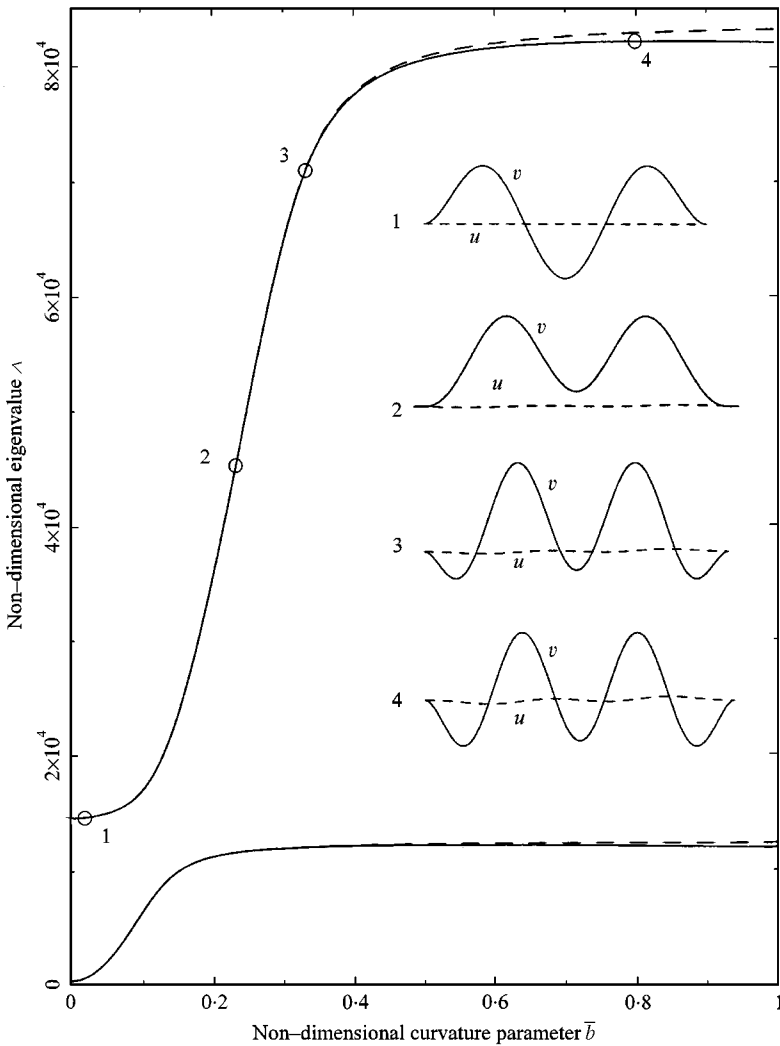


Figure 2. Numerical solution (———) and zeroth order analytic approximation ( – – – –) for the non-dimensional eigenvalue $\Lambda$ versus non-dimensional curvature parameter $\bar{b}$ (in this case $\bar{b} = \bar{\kappa}$) for the lowest two symmetric modes of a beam with constant curvature; $\varepsilon = 10^{-6}$. Mode shapes at progressively increasing curvature (corresponding to the marked points) are also shown.
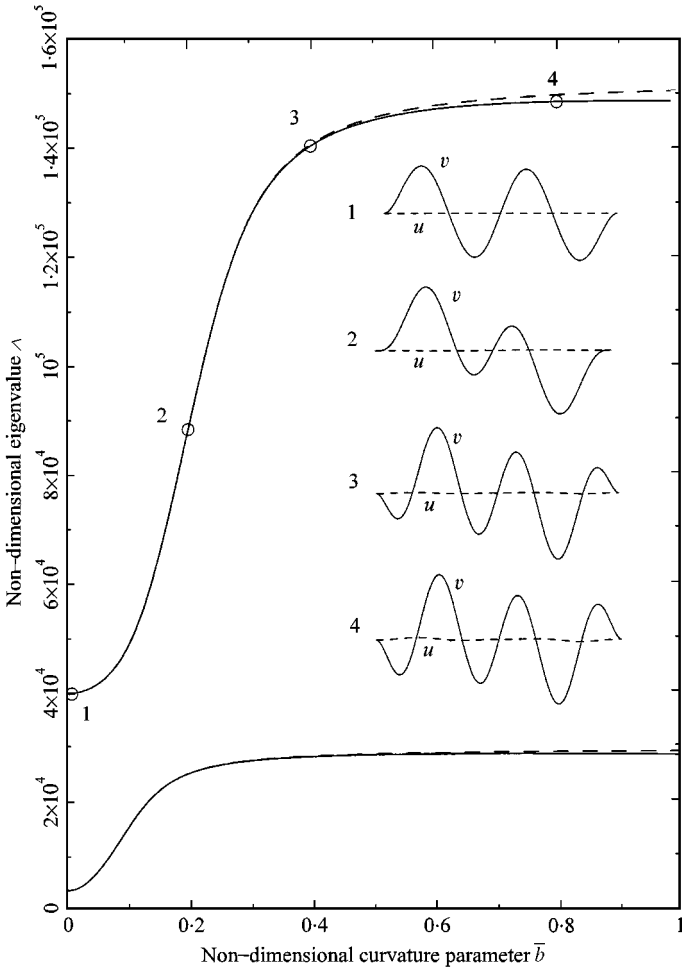
Figure 3. Numerical solution (——) and zeroth order analytic approximation (– – – –) to the non-dimensional eigenvalue $\Lambda$ versus non-dimensional curvature parameter $\bar{b}$ (in this case $\bar{b} = \bar{\kappa}$) for the lowest two symmetric modes of a beam with antisymmetric linear curvature; $\varepsilon = 10^{-7}$. Mode shapes corresponding to the marked points are also shown in the plot.

beam. The mode shape during the transition stage gains an additional component which is proportional to the beam curvature function (this component is a constant for a beam with constant curvature and is an antisymmetric linear function for a beam with antisymmetric linear curvature). We also can see that, as predicted analytically in Section 3, this additional component remains in the mode shape even after the completion of the mode transition, when the vibration is converted into a nearly inextensional one.

The similarity and distinctions between the low and high mode-number transition are summarized in Table 1.

To illustrate the validity of the zeroth order approximation for thicker beams, it is convenient to plot the non-dimensional eigenvalue $\Lambda$ versus the scaled non-dimensional curvature parameter $\hat{b}$ (Figure 4). It can be seen that zeroth order

Table 1

*Similarities and distinctions between high and low mode-number vibrational behaviour*

| High mode-number transition | Low mode-number transition |
| --- | --- |

*Similar features*

1. Transition from a flexural mode of a straight beam through the extensional stage into an inextensional mode
2. Composite structure of mode shape during the transition stage

| *Distinctions* | |
| --- | --- |
| 1. At the end of the transition stage, the eigenvalue increases to | |
| the eigenvalue of the next mode (with the same symmetry) of a straight beam | the asymptotic limit that is lower than the eigenvalue of the next mode (with the same symmetry) of a straight beam |
| 2. Additional component that appears in the transverse displacement during the transition stage | |
| is the solution of membrane vibration problem | is proportional to the beam curvature (for curvature functions represented by polynomial up to third degree) |
| 3. At the end of the transition stage, the mode shape | |
| is similar to the one of the next higher mode of a straight beam | contains an additional component which is a function of beam curvature |

approximation is adequate for part of the transition stage even for relatively thick beams. However, the completion of the transition stage cannot be described by the zeroth order approximation and a higher order approximation is required.

A comparison of the first order approximation with an exact numerical solution of equations (1) and (2) for beams with uniform curvature is shown in Figure 5 for several values of the slenderness parameter $\varepsilon$. Clearly, the first order approximation adequately describes the frequency throughout the transition stage for much thicker beams (with thickness to length ratio up to $5 \times 10^{-2}$). Higher order approximations are required to describe the frequency throughout the whole transition stage for even thicker beams. The first order approximation also reveals that, after the mode transition stage which is accompanied by an increase in frequency, a stage follows in which the frequency decreases. This stage, as well as the vibrational behaviour of beams with arbitrarily large curvature, will be investigated in a separate paper [12].

## 5. PHYSICAL INTERPRETATION

It is helpful to have a physical interpretation of the results of our analytical calculations, and particularly of the mode transitions and other features shown in
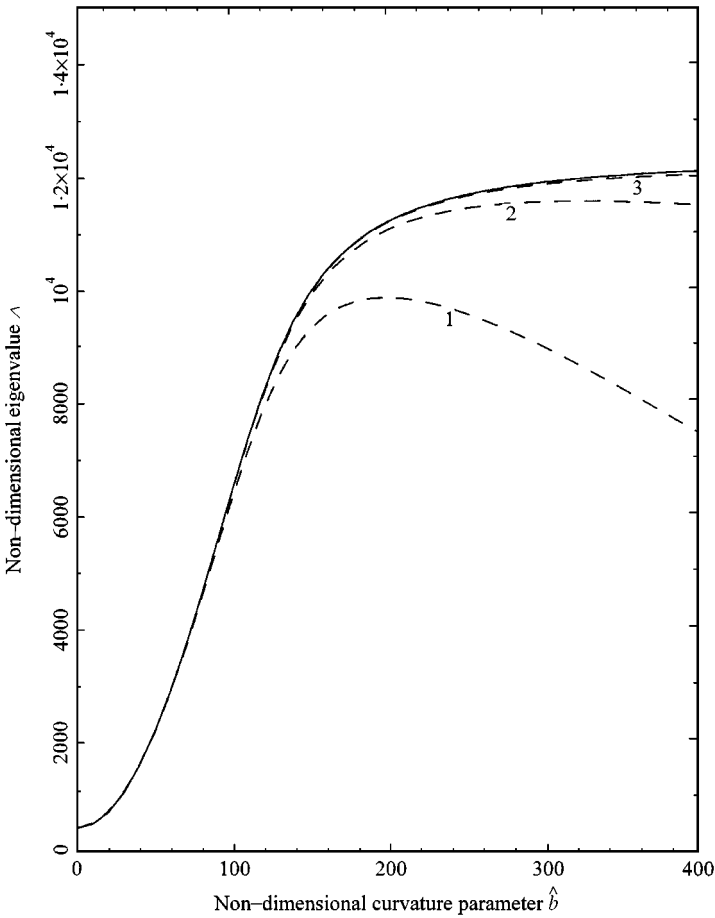
Figure 4. Zeroth order approximation (——) and numerical solution (– – – –) for the lowest symmetric mode of a beam with constant curvature plotted as functions of $\hat{b} = \hat{\kappa} = \kappa l \varepsilon^{-1/2}$; 1: $\varepsilon = 10^{-4}$, 2: $\varepsilon = 10^{-5}$, 3: $\varepsilon = 10^{-6}$.

the figures. To do this we use a rather different notation from that in the rest of the paper, but point out the connections.

In the first place, we note once again that, provided the curvature function is either symmetric or antisymmetric about the mid-point of the beam, the mode functions divide into two classes of odd and even symmetry respectively. There is no interactions between the two classes, and they can be treated separately. For clarity, therefore, we confine our attention to the case of constant (symmetric) curvature, and discuss other cases later. The aim is to examine the changes in the mode function and mode frequencies as the curvature is gradually increased from zero. In particular, we shall use the Rayleigh–Ritz vibrational approach [13] to determine the behaviour of the lowest symmetric mode, and then show how this treatment can be extended to other modes.

The Rayleigh–Ritz method involves expressing a trial mode function as a series of orthogonal functions with the coefficients as variational parameters, and shows that the energy derived using such trial function is always greater than or equal to
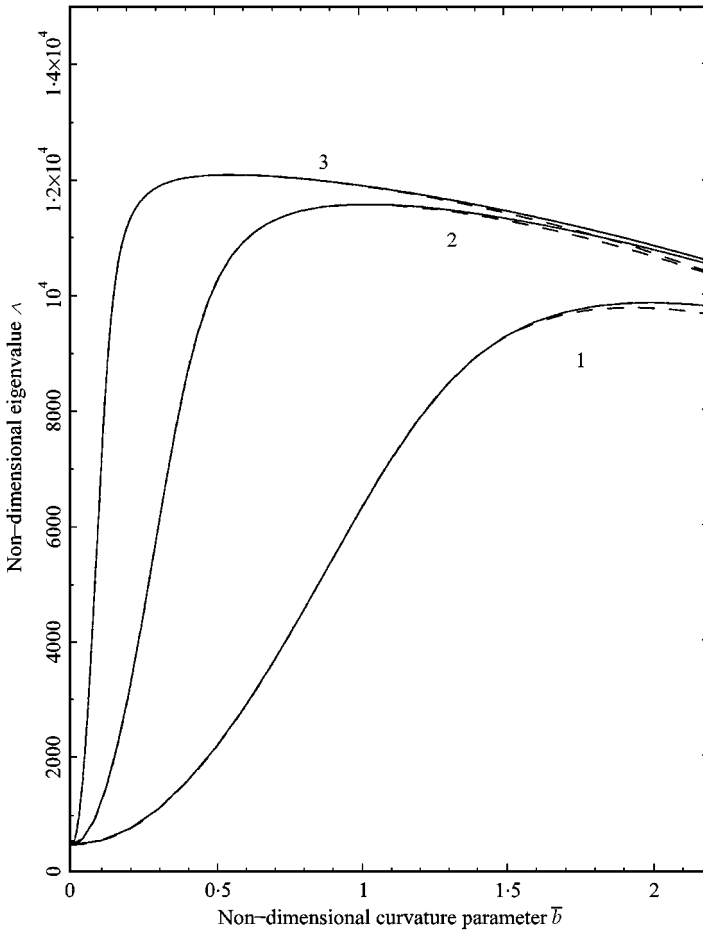
Figure 5. Numerical solution (———) and first order approximation (– – – –) for non-dimensional eigenvalue $\Lambda$ versus non-dimensional curvature parameter $\bar{b}$ ($\bar{b} = \bar{\kappa} = \kappa l$) for the lowest symmetric mode of a beam with constant curvature; 1: $\varepsilon = 10^{-4}$, 2: $\varepsilon = 10^{-5}$, 3: $\varepsilon = 10^{-6}$.

the exact mode energy. Suppose that $v_n^0(s)$ are the normalized mode functions for transverse displacements of a clamped straight beam. Then, since these form a complete orthonormal set, the transverse mode functions $v_n$ for the curved beam can be expressed in terms of them. In general, we should choose a similar set of orthogonal functions to represent the longitudinal displacements but, for the low-frequency modes of a thin beam, as considered here, it is valid to make the approximation that the tension is constant along the beam. The tangential displacement $u_n$ for the transverse mode $n$ is therefore uniquely determined in terms of the associated transverse displacement $v_n$ and the curvature function $\kappa$, which in this case is constant. Our initial aim is to examine the behaviour of the lowest symmetric mode as a function of curvature.

For small oscillations of a curved beam, we know that the time-averaged kinetic energy is equal to the time-averaged potential energy for the whole beam. The kinetic energy can be separated into two parts, $T_T$ and $T_L$ respectively,

corresponding to transverse and longitudinal motion. The potential energy can be similarly divided into the strain energy of bending, $V_B$, and the strain energy of extension, $V_E$. The energy equality for a mode $(u, v)$ of the curved beam can therefore be written symbolically in the form $T_T + T_L = V_B + V_E$, from which we can derive the mode frequency $\omega$ as

$$\omega^2 = \frac{\int (v\mathscr{L}_B v + u\mathscr{L}_E u)\,\mathrm{d}s}{m\int (v^2 + u^2)\,\mathrm{d}s}, \qquad (58)$$

where $\mathscr{L}_B$ and $\mathscr{L}_E$ are linear differential operators that give the bending and extensional forces, respectively, when operating on a mode functions, and $m$ is the mass of the beam. By the Rayleigh–Ritz principle [13], the frequency calculated from (58) for any trial transverse mode function $v(s)$ and its associated longitudinal function $u(s)$ will be greater than or equal to the true ground-state frequency. The frequency $\omega$ of the lowest mode can therefore be estimated by varying the coefficients that express the trial transverse mode function $v(s)$ in terms of the straight-beam function $v_n^0(s)$ so as to minimize $\omega$.

If we choose $v = v_1^0$ as the trial function, then geometry, and the condition of constant tension, dictate a longitudinal function $u$, the magnitude of which is proportional to the scaled curvature $\bar{\kappa} = \kappa l$ and also proportional to the magnitude of $v$. For small curvature, $u \ll v$ and so can be neglected in the denominator of equation (58), but the extensional energy term is significant and must be retained in the numerator. This leads to a result of the from

$$\omega^2 = \omega_1^2 + \alpha\bar{\kappa}^2, \qquad (59)$$

where $\alpha$ is a constant and $\omega_1$ is the first-mode frequency for a straight beam. Expression (59) then represents an upper bound to the true ground-state frequency, and is actually close to the true picture, as shown by the initial frequency rise in Figure 2.

For a larger uniform curvature, the variational approach is used and an admixture of higher modes $v_n^0$ with $n > 1$ must be considered. Suppose the sign of all the unperturbed symmetric mode functions is chosen so that they cause a net tension in the curved beam. Then, from the odd number of half-wavelengths in the unperturbed functions, we can see that this extension varies approximately as $1/n$, where $n$ is the mode number. It therefore makes sense to try a variational function of the form $v = Av_1^0 + Bv_3^0$ where mode 3 is the second straight-beam symmetrical mode with frequency $\omega_3$ and $A$ and $B$ are variational coefficients. If $B$ is chosen so that $B \approx -3A$, then the net extension for the variational function will be zero and, from equation (58), the frequency of the perturbed mode will be given by

$$\omega^2 \approx \frac{A^2\omega_1^2 + B^2\omega_3^2}{A^2 + B^2}$$

$$\approx \omega_1^2 + \frac{9(\omega_3^2 - \omega_1^2)}{10}. \qquad (60)$$

In this limit, therefore, there has been a modification to mode 1 by addition of a large amount of next symmetric mode 3, and the mode frequency has shifted to

a little below that of mode 3. In a proper variational calculation, the possibility of admixtures of higher modes would be considered, but the mode 3 addition will dominate because of the bending-energy penalty associated with higher modes.

In accord with the Rayleigh–Ritz principle, the true ground-state frequency lies below the two curves given by equation (59) and (60). There is, of course, a smooth transition between these two cases, as is shown in Figure 2.

This approach can be extended to higher symmetric modes by eliminating the modified mode 1 function from the set of available variational functions by imposing an appropriate condition on the first two expansion coefficients so as to ensure orthogonality of the new variational function to the ground-state function. The squared frequency of mode 3 then initially rises quadratically with curvature, as for mode 1, and settles down at a value a little below $\omega_5$.

This approach can also be extended to symmetric curvatures other than those that are constant, in which case there will still be a frequency increase followed by mode mixing, but the quantitative details may be very different.

When antisymmetric modes are considered in the symmetric-curvature case, it is clear that they produce no nett extension. This means that the frequencies of such modes are unaffected by curvature, and the mode-mixing phenomenon does not occur. Exactly the opposite situation pertains when the beam curvature is antisymmetric: in that case, antisymmetric modes suffer frequency increase followed by mode mixing, as shown in Figure 3, while symmetric modes are unaffected by curvature. If the curvature is neither symmetric nor antisymmetric, then all modes increase in frequency as the curvature is increased, and for larger curvature there is mode mixings between all modes, and not just those of the same symmetry type.

Figure 5 shows a further feature of the behaviour, in that the rate at which the frequency rises with curvature depends upon the thickness parameter $\varepsilon$, thicker beams changing frequency less than thinner beams. The reason for this is immediately apparent from equation (58), for the elastic energy of bending $V_B$ varies as $\varepsilon^2 v^2$ while the elastic energy of extension varies as $\varepsilon u^2$ or $\varepsilon \bar{\kappa}^2 v^2$. This means that the parameter determining the initial effect of curvature on the mode frequency is $\bar{\kappa}^2/\varepsilon$, so that the initial effect of curvature $\bar{\kappa}$ scales as $\varepsilon^{1/2}$. This conclusion is in good agreement with the initial parts of the plots in Figure 5, and indeed the initial parts of all plots coincide if the horizontal axis is scaled in terms of $\hat{\kappa}$, as in Figure 4, rather than $\bar{\kappa}$. This change, however, destroys the overlap of the plots at higher curvatures.

From Figure 5, it is also clear that a new phenomenon enters when the curvature becomes larger, for the frequencies of all modes then begin to decline. This is also easily understood in terms of the discussion above. In the first place, the discussion has neglected the contribution of the longitudinal motion $u$ to the kinetic energy in equation (58). This neglect is justified when $\bar{\kappa} \ll 1$, since $u$ is of order $\bar{\kappa}v/(n+2)$ for the transformed mode $n$, but ceases to be valid for greater curvatures. When the kinetic energy associated with longitudinal motion is included in the calculation, it reduces the predicted frequency correspondingly. The predicted result is that, instead of $\omega$ reaching a plateau just below $\omega_{n+2}$, it will become

asymptotic to the curve

$$\omega^2 \approx \frac{(n+2)^2 \omega_{n+2}^2}{(n+2)^2 + \bar{\kappa}^2} \tag{61}$$

for large $\bar{\kappa}$. At a given value of scaled curvature $\bar{\kappa}$, the relative effect on mode frequency is independent of the thickness parameter $\varepsilon$, though the effect of this on the frequency curves must be interpreted in the light of the discussion in the previous paragraph. This agrees with the behaviour shown in Figure 5. This decrease in mode frequency at larger curvatures occurs independently of the symmetries of the modes or of the curvature function. It is discussed in more detail in another paper [12].

## 6. CONCLUSIONS

Analysis of the low-frequency free in-plane vibration of beams with arbitrarily varying curvature and cross-section and clamped ends reveals that, depending on the type of symmetry of the beam curvature and cross-section, with increase in non-dimensional curvature $\bar{\kappa}$ (where $\bar{\kappa} = \kappa l$) some modes undergo a transition from the flexural mode of a straight beam, through an extensional stage, into a nearly inextensional mode that resembles the next higher flexural mode (with the same symmetry) of a straight beam.

The main results of the paper can be summarized as follows:

1. A simple integral condition which shows which modes undergo a transition for a particular type of beam curvature and cross-section is obtained.
2. Many features of the low-frequency mode transition are revealed analytically. This includes the effect of beam curvature on mode shape during the transition stage and an expression for the asymptotic limit for frequency at the end of the transition stage.
3. The analysis reveals that although there is similarity between the low mode-number transition and high mode-number transition examined in a previous paper by the present authors [11], there are also significant distinctions between them. The similarities and distinctions are presented in Table 1.
4. Analytic approximations (zeroth order) for frequency and mode shape have been derived for the cases of beam curvature represented by symmetric and antisymmetric polynomial functions. The approximations describe sufficiently accurately the entire transition stage for relatively thin beams (with thickness to length ratio of $5 \times 10^{-3}$ and smaller).
5. A higher order analytic approximation that describes the vibrational behaviour in the transition region for much thicker beams has been derived using the case of a uniformly curved beam as example. This approximation shows that, after the initial mode transition stage which is accompanied by an increase in frequency, a stage of decrease in frequency follows. This stage as well as vibrational behaviour at arbitrarily large curvature will be discussed in a separate paper [12].

The properties of beam vibrational behaviour found by analytical study are confirmed by two numerical examples.

Although for the sake of simplicity the analysis has been confined to beams with clamped ends and with curvature function represented by symmetric or antisymmetric polynomials up to third degree, it is straightforward to extend it to the beams with hinged ends and to some other types of curvature functions.

## REFERENCES

 1. J. P. CHARPIE and C. B. BURROUGHS 1993 *Journal of the Acoustical Society of America* **94**, 866–879. An analytic model for the free in-plane vibration of beams of variable curvature and depth.
 2. R. H. GUTIERREZ, P. A. A. LAURA, R. E. ROSSI, R. BERTERO and A. VILLAGGI 1989 *Journal of Sound and Vibration* **129**, 181–200. In-plane vibrations of non-circular arcs of non-uniform cross-section.
 3. T. SAKIYAMA 1985 *Journal of Sound and Vibration* **102**, 448–453. Free vibrations of arches with variable cross section and non-symmetrical axis.
 4. P. A. A. LAURA and P. L. VERNIERE DE IRASSAR 1988 *Journal of Sound and Vibration* **124**, 1–12. A note on in-plane vibrations of arch-type structures of non-uniform cross-section: the case of linearity varying thickness.
 5. M. KAWAKAMI, T. SAKIYAMA, H. MATSUDA and C. MORITA 1995 *Journal of Sound and Vibration* **187**, 381–401. In-plane and out-of-plane free vibrations of curved beams with variable sections.
 6. A. BENEDETTI, L. DESERI and A. TRALLI 1996 *Journal of Engineering Mechanics* **122**, 291–299. Simple and effective equilibrium models for vibration analysis of curved rods.
 7. K. SUZUKI, S. TAKAHASHI and H. ISHIYAMA 1978 *Bulletin of the Japan Society of Mechanical Engineers* **21**, 618–627. In-plane vibrations of curved bars.
 8. K. SUZUKI and S. TAKAHASHI 1982 *Bulletin of the Japan Society of Mechanical Engineers* **25**, 1100–1107. In-plane vibrations of curved bars with varying cross-section.
 9. M. PETYT and C. C. FLEISCHER 1971 *Journal of Sound and Vibration* **18**, 17–30. Free vibration of a curved beam.
10. J. F. M. SCOTT and J. WOODHOUSE 1992 *Philosophical Transactions of the Royal Society of London, Physical Sciences and Engineering* **339**, 587–625. Vibration of an elastic strip with varying curvature.
11. T. TARNOPOLSKAYA, F. R. DE HOOG, N. H. FLETCHER and S. THWAITES 1996 *Journal of Sound and Vibration* **196**, 659–680. Asymptotic analysis of the free in-plane vibrations of beams with arbitrarily varying curvature and cross-section.
12. T. TARNOPOLSKAYA, F. R. DE HOOG, A. TARNOPOLSKY and N. H. FLETCHER 1999 *Journal of Sound and Vibration*. Vibration of beams and helices with arbitrarily large uniform curvature (submitted).
13. P. M. MORSE and H. FESHBACH 1953 *Methods of Theoretical Physics*, Vol. 2, 1117–1119. New York: McGraw-Hill.
14. U. ASCHER, J. CHRISTIANSEN and R. D. RUSSEL 1981 *Association for Computing Machinery Transaction on Mathematical Software* **7**, 209–222. Collocation software for boundary-value ODEs.